Electronic Supplementary Material (ESI) for Nanoscale.

Supporting Information

Exceptionally Large Fracture Strength and Stretchability of 2D ReS_2 and $ReSe_2$

Guy Alboteanu and Assaf Ya'akobovitz

Force-deflection measurements

We acquired more than 100 force-deflection measurements for each of the investigated materials. In addition to the measurements shown in Fig. 3d in the main text, we show some representative measurements in Fig. S1. We presented the distribution of all captured Young's moduli in Fig. S2. Notably, the averaged values of Young's moduli are given in Fig. 4a and b in the main text. The relationship between Young's moduli and pretension values of ReS_2 and $ReSe_2$ is shown in Fig. S3.

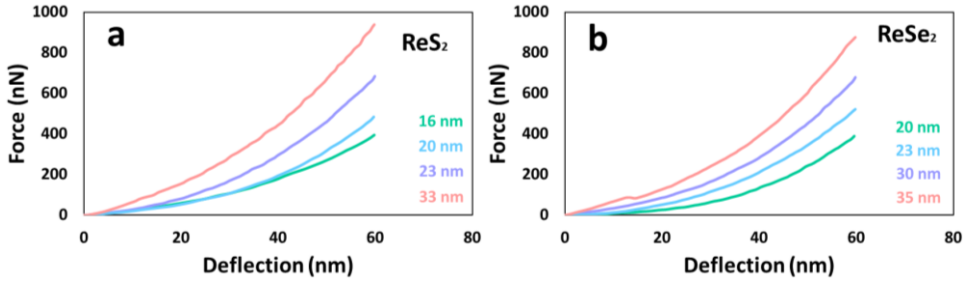

Fig. S1. Representative force-deflection measurements of (a) ReS_2 and (b) $ReSe_2$.

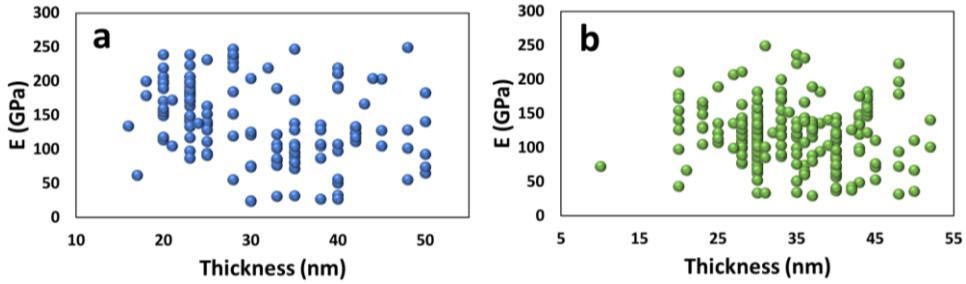

Fig. S2. Measured Young's moduli of (a) ReS_2 and (b) $ReSe_2$.

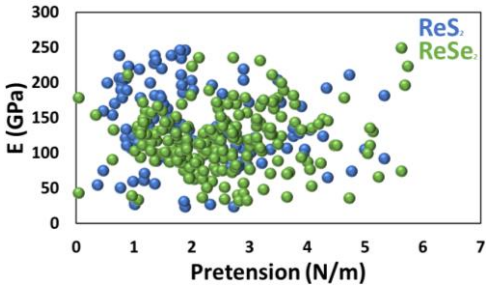

Fig. S3. The relationship between Young's modulus and pretension.

Studies included in Figure 6

The studies included in Fig. 6 in the main text are listed in Table S1.

Table S1. Studies included in Fig. 6 in the main text.

	Material	Thickness (nm)	Reference
Topological insulator	Bi_2Te_3	5	L. Guo, H. Yan, Q. Moore, M. Buettner, J. Song, L. Li, P. T. Araujo and H. Wang, *Nanoscale*, 2015, 7, 11915–11921.
Group III Mono-chalcogenides	GaS GaSe GaTe	10	B. Chitara and A. Ya'akobovitz, *Nanoscale*, 2018, 10, 13022– 13027.
TMDs	WSe_2	3.35	R. Zhang, V. Koutsos, R. Cheung, R. Zhang, V. Koutsos and R. Cheung, *Appl. Phys. Lett.*, 2016, 108, 042104.
	MoS_2	0.67 1.34	S. Bertolazzi, J. Brivio and A. Kis, *ACS Nano*, 2011, 12, 9703–9709.
	HS_2 HSe_2	12 14 13 15	Y. M. Jahn and A. Ya'akobovitz, *Nanoscale*, 2021, 13, 18458–18466.
Graphene	Gr	0.335	C. Lee, X. Wei, J. W. Kysar and J. Hone, *Science*, 2008, 321, 385–389.
Black phosphorus	BP	14.3-34	J.-Y. Wang, Y. Li, Z.-Y. Zhan, T. Li, L. Zhen and C.-Y. Xu, *Appl. Phys. Lett.*, 2016, 108, 013104.

Fracture measurements

We present additional representative fracture measurements in Fig. S4. All measured fracture strengths and maximal strains and their distributions are shown in Fig. S5 and Fig. S6, respectively.

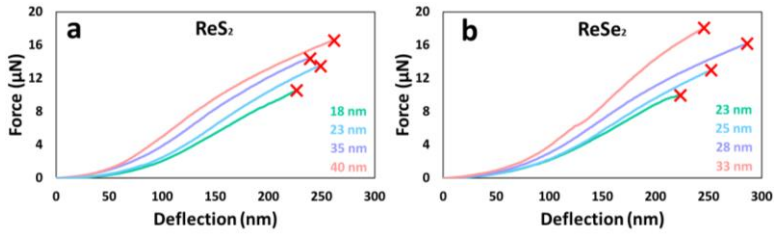

Fig. S4. Representative force-deflection measurements reaching fracture of (a) ReS_2 and (b) $ReSe_2$.

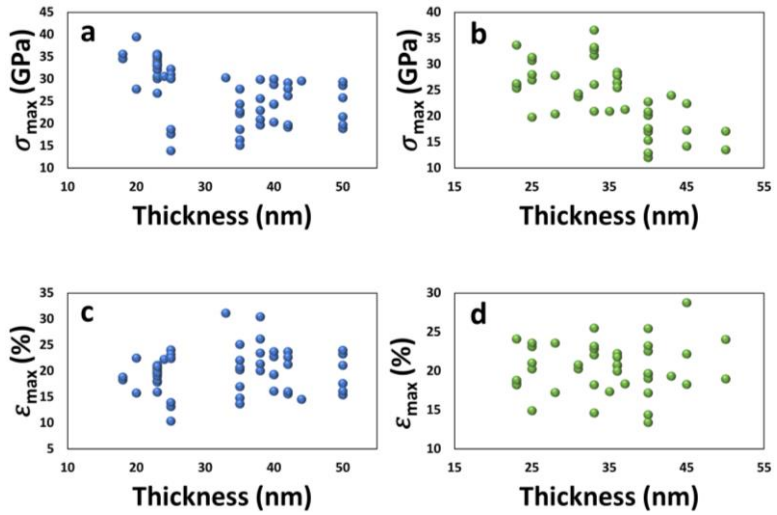

Fig. S5. Measured fracture strengths of (a) ReS_2 and (b) $ReSe_2$ nano-drumheads. Maximal strain measurements of (c) ReS_2 and (d) $ReSe_2$ nano-drumheads.

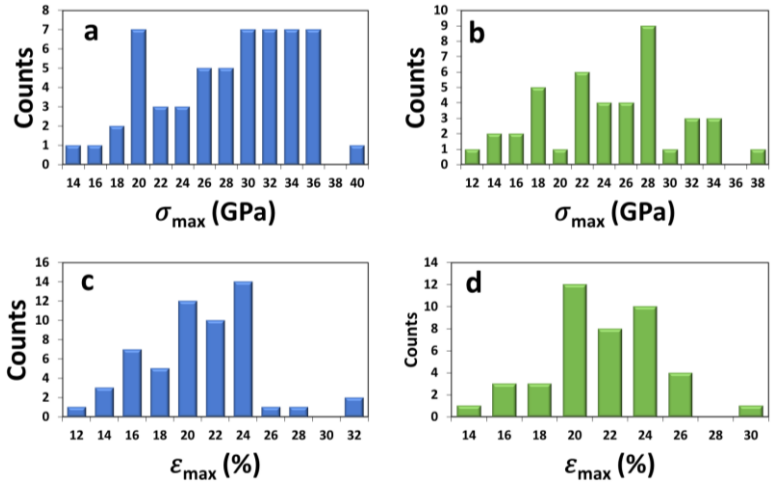

Fig. S6. Fracture strengths distribution of (a) ReS_2 and (b) $ReSe_2$. Maximal strain distributions of (c) ReS_2 and (d) $ReSe_2$.